

Supporting Information

Improved performance of solution processed OLEDs using N-annulated perylene diimide emitters with bulky side-chains

Sergey V. Dayneko,^{a,b} Edward Cieplechowicz,^a Sachin Suresh Bhojgude,^a Jefferey Van Humbeck,^a Majid Pahlevani,^{c*} Gregory C. Welch^{a*}

^a Department of Chemistry, University of Calgary, 731 Campus Place NW, Calgary, Alberta, Canada T2N 1N4

^b Genoptic LED Inc., 6000 72nd Avenue SE, Calgary, AB, Canada T2C 5C3

^c Department of Electrical and Computer Engineering, Queen's University, 19 Union St., Kingston, ON, Canada, K7L 3N6

*E-mail: majid.pahlevani@queensu.ca, gregory.welch@ucalgary.ca

TABLE OF CONTENTS

| | |
|--------------------------|-----|
| Materials and Methods | S2 |
| Optical Characterization | S4 |
| Synthetic Details | S6 |
| Electrochemistry | S30 |
| Extra OLED plots | S31 |
| References | S32 |

1. Materials and Methods

Materials: All chemicals/solvents were purchased from Millipore-Sigma and used without further purification. PFO was purchased from Ossila. Compound PDI-1, PDI-2 and PDI-3¹⁻³ were synthesized following the literature procedure. Chromatography was performed on silica gel (230-400 mesh) by standard techniques.

Colloidal ZnO nanocrystals: Colloidal ZnO nanocrystals were synthesized by a low-temperature solution-precipitation method⁴ with some modifications. A DMSO solution (30 ml) of zinc acetate hydrate (3 mmol) was prepared and an ethanol solution (10 ml) of TMAH (5.5 mmol) was added dropwise. The reaction mixture was stirred for one hour under ambient conditions. Then the ZnO nanocrystals were precipitated by adding ethyl acetate and redispersed in methanol. Additional ligands of 2-ethanolamine (160 μ l) was introduced to stabilize the nanoparticles. The solutions were filtered before use.

Nuclear Magnetic Resonance (NMR): ¹H and ¹³C NMR spectra were recorded on Bruker CIF-600 MHz, Bruker Ascend 500 MHz, and Bruker Fourier 300 MHz in solvents as indicated. Chemical shifts (δ) are given in ppm. The residual solvent signals were used as references and the chemical shifts converted to the TMS scale (CDCl₃: δ H = 7.26 ppm, δ C = 77.16 ppm).

High-resolution Mass Spectrometry (HRMS): High-resolution MALDI mass spectrometry measurements were performed courtesy of Jian Jun Li in the Chemical Instrumentation Facility at University of Calgary. A Bruker Autoflex III Smartbeam MALDI-TOF (Na:YAG laser, 355nm), setting in positive reflective mode, was used to acquire spectra. Operation settings were all typical, e.g. laser offset 62-69; laser frequency 200Hz; and number of shots 300. The target used was Bruker MTP 384 ground steel plate target. Sample was dissolved in an appropriate solvent and mixed with matrix solution (α -Cyano-4-hydroxycinnamic acid/MeOH). The concentration of ratio of sample to matrix is approximately 1:100.

CHN Analysis: Elemental analysis was performed by Jian Jun Li in the Chemical Instrumentation Facility at the University of Calgary. A Perkin Elmer 2400 Series II CHN Elemental Analyzer was used to obtain CHN data.

UV-Visible Spectroscopy (UV-Vis): All optical absorption measurements were recorded using Agilent Technologies Cary 60 UV-Vis spectrometer at room temperature. Films were spin-cast into Corning glass micro slides. Prior to use, glass slides were cleaned with soap and water, acetone and isopropanol, and followed by UV/ozone treatment using a Novascan UV/ozone cleaning system.

Cyclic Voltammetry (CV): Electrochemical measurements were performed using a CH Instruments Inc. Model 1200B Series Handheld Potentiostat. A standard 3-electrode setup was utilized, consisting of a freshly polished glassy carbon disk working electrode (WE), Pt-wire counter electrode (CE), and Ag-wire pseudo-reference electrode (RE). All measurements were referenced to ferrocene/ferrocenium (Fc/Fc⁺) as internal standard. All cyclic voltammetry experiments were performed at a scan rate of 100 mV/s. Sample solutions, with 1 mM compound and 0.1 M tetrabutylammonium hexafluorophosphate (TBAPF₆) supporting electrolyte, were prepared in anhydrous dichloromethane. All electrochemical solutions were sparged with dry gas (either N₂ or argon) for 5 minutes to deoxygenate the system prior to measurements.

OLEDs Device Fabrication and Testing: OLED devices were fabricated on ITO-coated glass substrates (sheet resistance of 10 Ohm Sq⁻¹), which were first cleaned by sequentially ultrasonicating detergent and de-ionized water, acetone and isopropanol before use. Glass/ITO substrates were first pretreated under UV-ozone for 30 minutes. PEDOT:PSS aqueous suspension was spin-coated onto the ITO-coated glass substrates at 3,000 rpm for 60s and annealed in air at 150°C. PVK dissolved in toluene (10 mg mL⁻¹) was spin-coated at 3000 rpm for 60 s and baked at 120 °C for 10 min. For deposition of the PFO:PDI emitter layer, the blend solution of PFO:PDI (ratio 2:18 at total concentration of 10 mg mL⁻¹) dissolved in *o*-xylene was spin-cast at 2,000 rpm on top of the PVK layer and annealed in air at 150°C for 30 min. Then, the ZnO nanoparticles (20 mg mL⁻¹ in methanol) were spin-cast at 4,000 rpm on top of the emitter layer and annealed in air at 80°C. Finally, the Ag (100 nm) electrode was deposited using a thermal evaporation system through a shadow mask under a base pressure of $\sim 2 \times 10^{-6}$ torr. The device area was 9 mm² as defined by the overlapping area of the ITO films and top electrodes. Current density-voltage (J-V) characteristics were measured using a Keithley 2612B source-meter combined with calibrated Si-photodiode and spectrometer^{5,6}.

Absolute PLQY measurements and re-absorption correction: Absolute PLQY measurements of all samples were performed by using an integrating sphere accessory on a fluorimeter⁷. All spectra for the absolute quantum yield measurements were corrected for the light source noise, wavelength sensitivity and the transmittance. To calculate PLQY has been used the equation:

$$PLQY_{obs} = \frac{E_c - E_a}{L_a - L_c}$$

where E_c and E_a – integral of emission spectra with and without sample in the integrated sphere and L_c and L_a – integral of excitation spectrum with and without sample in the integrated sphere.

The re-absorption correction was used on all films PLQY measurement. First, denoting the scaled molecular emission spectrum by $E'(\lambda)$ and the observed emission spectrum $E_{obs}(\lambda)$, a self-absorption coefficient α , can be calculated from:

$$\alpha = 1 - \frac{\int E_{obs}(\lambda)d\lambda}{\int E'(\lambda)d\lambda}$$

The re-absorption has been calculated by using observed PLQY and self-absorption coefficient α in next equation:

$$PLQY_{corr} = \frac{PLQY_{obs}}{1 - \alpha + \alpha PLQY_{obs}}$$

2. Optical Characterization

Solvent resistance: It is known that to make a high-performance OLED device by solution processing methods, uniform film formation and film stability is critical, and thus the solvent resistance is important each layer. To choose the best solvent for processing the ZnO nanoparticles on top of the PDI films without destroying the PDI films we examined three different solvents (ethanol, isopropyl alcohol and methanol) which could dissolve the ZnO NPs. The films of PDI-1, PDI-2 and PDI-3 were spin-cast at 2,000 rpm from *o*-xylene on glass substrates (2.5 x 2.5) cm and baked at 150°C for 30 min. The absorption spectra of as-cast PDI films is shown in Figures S1 and S2. To study the solvent resistance of the films, 200 μ L solution (ethanol, isopropyl alcohol, or methanol) was applied to the PDI film followed by rotating at 4,000 rpm to remove the solvent, this procedure repeated a 5-7 times. The absorption spectra of all PDI films after each exposure to alcohol is shown in Figure S1 and S2. A decrease in the absorption spectra of PDI-1 films after five times exposure to ethanol or isopropyl alcohol indicates degradation of the PDI-1 film via material removal. No significant changes to the PDI-1 film was seen when using methanol indicating good solvent resistance (Figure S1c). Films of PDI-2 and PDI-3 were subject to the same methanol exposure (Figure S2). PDI-3 films have solvent resistance where PDI-2 films show some degradation. This degradation only becomes significant after 3 coatings of methanol; thus the films are able to handle coating of one layer of ZnO NPs from methanol. We concluded that coating ZnO NPs from methanol is suitable to not destroy the PDI based emitting layers.

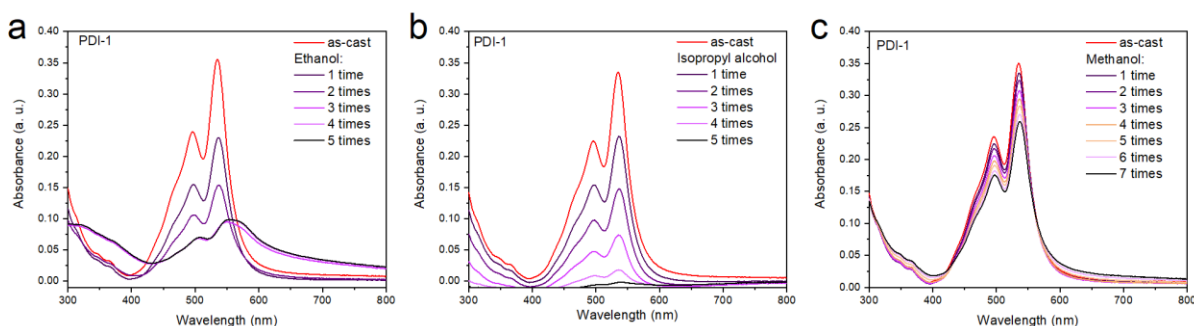


Figure S1. Solvent resistance tests for PDI-1 films. Absorption spectra recorded before and after coating solvents on top.

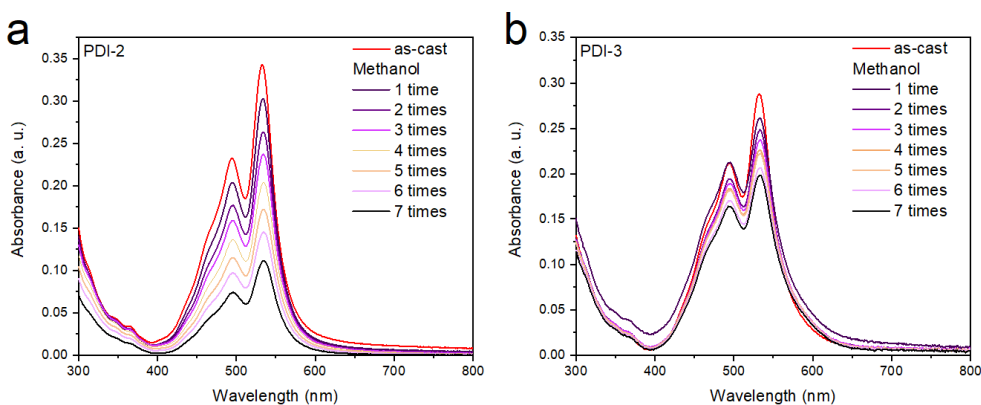


Figure S2. Solvent resistance tests for PDI-2 and PDI-3 films. Absorption spectra recorded before and after coating solvents on top.

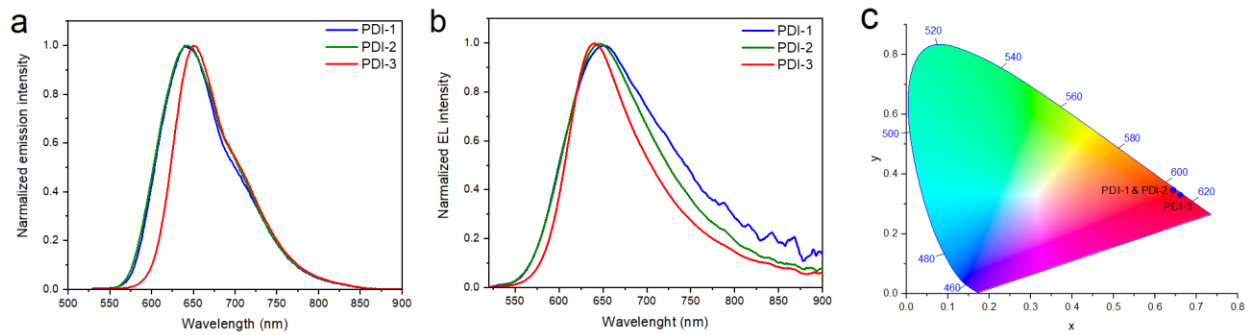
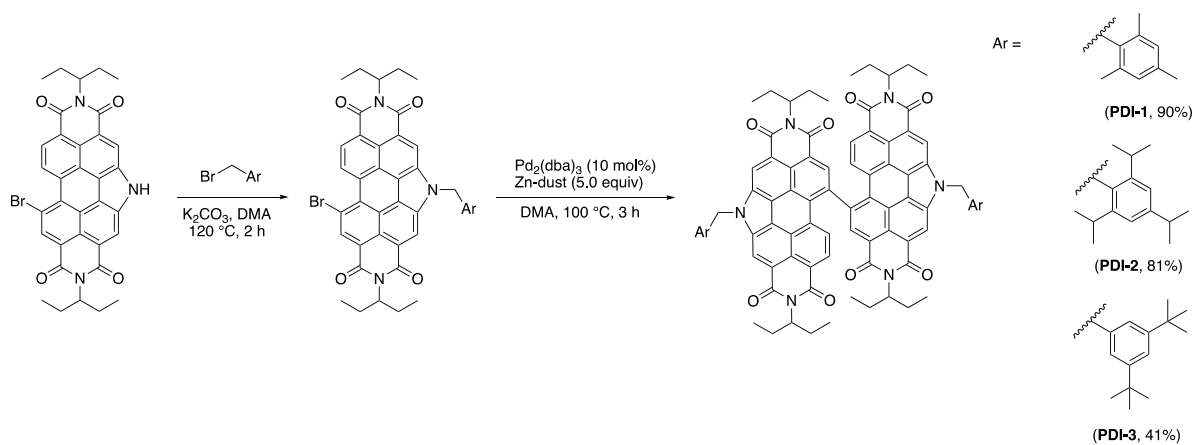
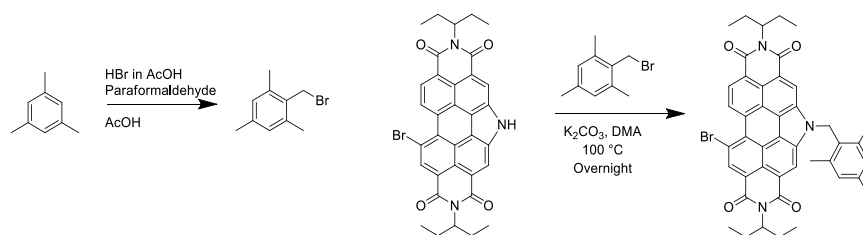


Figure S3. (a) PL, (b) EL spectra and (c) CIE coordinates of PDI based films.

2. Synthetic Details.

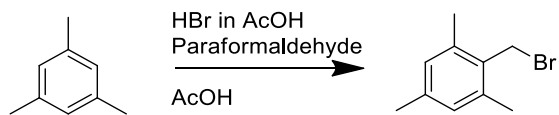


Scheme S1. Synthetic route towards PDI based materials.



Scheme S2. Synthetic route towards the trimethyl benzyl side chain and monomer.

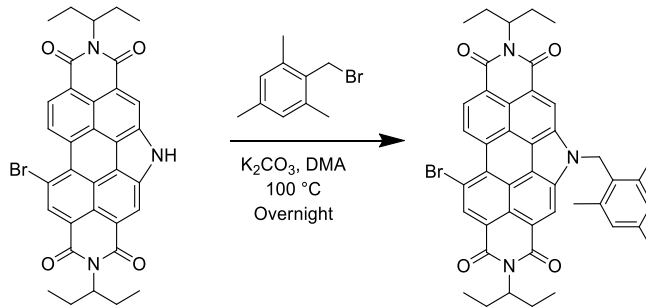
Synthesis of 1-(bromomethyl)-2,4,6-trimethylbenzene:



The following compound was prepared via literature procedure,³ the reaction was scaled down to 2.0 grams. Spectra data matched literature report. (2.58g, 74% yield)

¹H NMR (500 MHz, Chloroform-*d*) δ : 6.87 (s, 2H), 4.58 (s, 2H), 2.39 (s, 6H), 2.27 (s, 3H).

Synthesis of Br-PDIN-2,4,6-trimethylbenzyl:

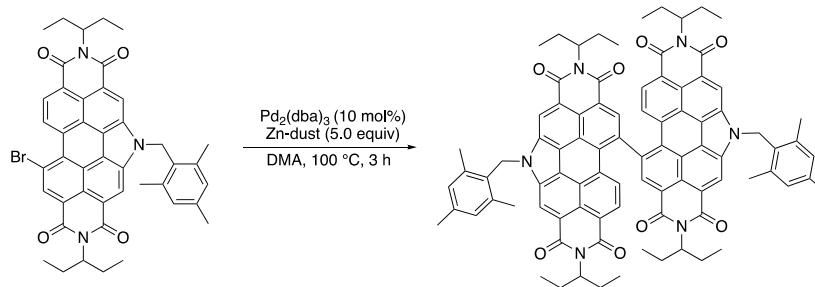


To a 250 mL round bottom flask equipped with a magnetic stir bar were added the **Br-PDIN-H** (1.26 g, 2.02 mmol), **1-(bromomethyl)-2,4,6-trimethylbenzene** (1.30 g, 6.10 mmol), and **K₂CO₃** (1.64 g, 11.9 mmol). 100 mL of *N,N*-Dimethylacetamide (DMA) solvent was added using a graduated cylinder and seal with a septa. The reaction mixture was sparged with nitrogen for 15 minutes. The reaction mixture was placed in an aluminum bead bath with stirring and heated to 100 °C overnight. The reaction mixture was cooled to room temperature and dissolved in 300 mL of DCM and washed with water (3 X 700 mL). The solvent was evaporated using rotary evaporation and the crude residue was again dissolved in DCM and passed through a short silica plug followed by elution with DCM. The DCM solution was poured into 500 mL of methanol, the DCM was removed using evaporated using rotary evaporation at 35 °C to yield an orange slurry in the methanol. The pure product was isolated *via* vacuum filtration, (1.45 g, 95% yield).

¹H NMR (300 MHz, Chloroform-*d*) δ : 10.04 (d, $J = 8.4$ Hz, 1H), 8.95 (s, 1H), 8.77 (d, $J = 8.4$ Hz, 1H), 8.59 (s, 2H), 7.06 (s, 2H), 6.07 (s, 2H), 5.16 (dt, $J = 9.3, 6.1$ Hz, 2H), 2.43 – 2.23 (m, 13H), 2.03 (dddd, $J = 13.7, 7.5, 6.2, 4.0$ Hz, 4H), 0.99 (td, $J = 7.4, 4.8$ Hz, 12H).

¹³C NMR (75 MHz, CDCl₃) δ : 165.67, 139.50, 137.98, 134.79, 134.60, 134.33, 132.17, 130.29, 130.23, 127.99, 127.22, 124.18, 123.55, 123.22, 122.23, 122.02, 121.17, 119.02, 118.76, 118.36, 77.58, 77.16, 76.74, 58.12, 57.96, 45.98, 25.29, 25.22, 21.27, 20.42, 11.73, 11.70.

Synthesis of PDI-1:



To a 40 mL screw-capped vial equipped with a magnetic stir bar were added the **Br-PDIN-3,5-di-tert-butylbenzyl** (1.1 g, 1.33 mmol), **zinc dust** (0.436 g, 6.67 mmol) and dried in a vacuum oven overnight at 80 °C. **Pd₂(dba)₃** (0.122 g, 0.13 mmol) was added inside the glove box and the vial was closed with a cap. 20.0 mL of dry DMA solvent was cannula transferred outside the glove box under nitrogen. The reaction mixture was placed in an aluminum bead bath with stirring and heated to 120 °C, after which the solution turned blue. TLC analysis showed starting material consumption after 3 h. The reaction mixture was cooled to rt, dissolved in DCM and passed through two Celite plugs to remove the zinc and Pd-catalyst. The solvent was evaporated using rotary evaporation, the crude residue was again dissolved in DCM and passed through a silica plug to remove the baseline spot observed by TLC analysis. The solvent was evaporated using rotary evaporation. The solid was purified by boiling in isopropanol for 1.5 h followed by vacuum filtration. This was performed twice to removed impurity observed by TLC analysis. This yielded a pure product, a bright orange powder (0.893g, 90% yield).

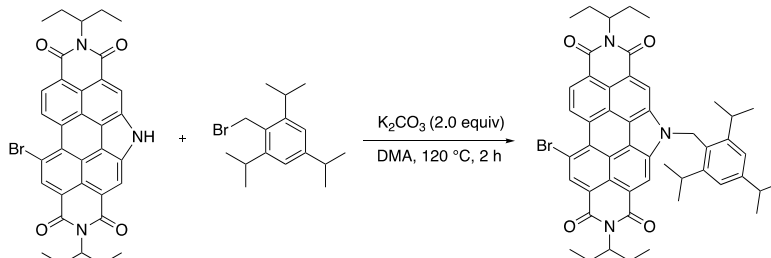
¹H NMR (500 MHz, Chloroform-*d*) δ : 8.84 (s, 4H), 8.68 (s, 2H), 7.94 (s, 2H), 7.67 (d, $J = 8.4$ Hz, 2H), 7.15 (s, 4H), 6.19 (s, 4H), 5.19 (s, 2H), 5.01 (s, 2H), 2.44 (d, $J = 4.2$ Hz, 19H), 2.37 – 2.26 (m, 4H), 2.16 (s, 4H), 1.98 (dq, $J = 13.7, 6.8, 6.3$ Hz, 4H), 1.84 (tt, $J = 13.5, 7.4$ Hz, 4H), 0.98 (t, $J = 7.0$ Hz, 14H), 0.81 (s, 14H).

¹³C NMR (75 MHz, CDCl₃) δ : 166.52, 165.21, 163.79, 140.91, 139.71, 138.20, 135.57, 135.41, 132.96, 130.42, 130.38, 129.13, 128.32, 128.01, 126.84, 125.04, 124.81, 123.59, 123.59, 122.77, 120.27, 119.94, 77.58, 77.36, 77.16, 76.74, 58.02, 57.64, 46.27, 25.27, 25.15, 25.10, 21.37, 20.47, 11.67, 11.60, 11.42.

MALDI-TOF: (m/z) calculated [M-2H]+H⁺ for C₈₈H₈₀N₆O₈: 1347.60, obtained: 1347.58

Elemental Analysis: Theory %C 78.31, %H 5.97, %N 6.23. Actual %C 77.26, %H 5.96, %N 6.19.

Synthesis of Br-PDIN-2,4,6-trisopropylbenzyl:



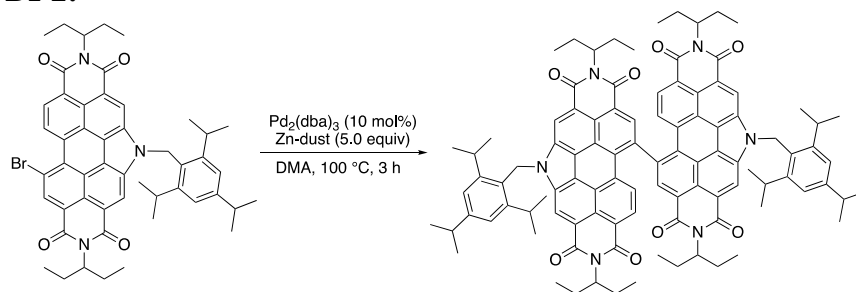
To a 20 mL screw-capped vial equipped with a magnetic stir bar were added the **Br-PDIN-H** (1.0 g, 1.60 mmol), **2,4,6-trisopropylbenzyl bromide** (0.620 g, 2.08 mmol), and **K₂CO₃** (0.443 g, 3.21 mmol). The screw-capped vial was closed and evacuated using high vacuum, then refilled with nitrogen gas in three cycles. To the vial 8.0 mL of *N,N*-Dimethylacetamide (DMA) solvent was added using syringe under nitrogen and reaction mixture purged with nitrogen for 10 minutes. The reaction mixture was placed in heating block with stirring and heated to 120 °C. TLC analysis showed reaction completion after 2 h, then the reaction mixture was cooled to rt and dissolved in 200 mL of DCM and washed with water (3 X 400 mL). The solvent was evaporated using rotary evaporation and the crude residue was again dissolved in DCM and passed through silica plug followed by elution with DCM. The DCM was removed and the product was recrystallized by dissolving in a minimal amount of DCM and precipitating with MeOH. The pure product was isolated *via* vacuum filtration, washing with methanol (1.145 g, 85% yield).

¹H-NMR (600 MHz, CDCl₃) δ: 10.09-10.07 (m, 1H), 8.94 (s, 1H), 8.79 (d, *J* = 8.0 Hz, 1H), 8.46 (s, 2H), 7.29 (s, 2H), 6.20 (s, 2H), 5.19-5.13 (m, 2H), 3.35-3.28 (m, 2H), 3.10-3.04 (m, 1H), 2.37-2.27 (m, 4H), 2.06-1.97 (m, 4H), 1.39 (d, *J* = 7.0 Hz, 6H), 1.12 (d, *J* = 6.8 Hz, 12H), 1.00-0.95 (m, 12H).

¹³C-NMR (150 MHz, CDCl₃) δ: 151.45, 148.98, 135.13, 134.94, 134.49, 132.65, 130.69, 127.56, 127.26, 125.22, 124.47, 123.96, 123.44, 122.45, 122.37, 121.36, 119.66, 119.23, 118.80, 58.00, 57.86, 44.51, 34.81, 30.42, 25.32, 25.25, 24.34, 24.20, 11.62, 11.59.

MALDI-TOF: (*m/z*) calculated [M-2H]⁺H⁺ for C₅₀H₅₂BrN₃O₄: 836.3057, obtained: 836.3075

Synthesis of PDI-2:



To a 40 mL screw-capped vial equipped with a magnetic stir bar were added the **Br-PDIN-2,4,6-trisopropylbenzyl** (1.5 g, 1.79 mmol), **zinc dust** (0.585 g, 8.94 mmol), and **Pd₂(dba)₃** (0.164 g, 0.17 mmol) inside the glove box and the vial was closed with a cap. The mixture was dissolved in 25.0 mL of DMA solvent outside the glove box under nitrogen. The reaction mixture was placed in heating block with stirring and heated to 100 °C, after which the solution turned blue. TLC analysis showed completion of reaction after 3 h. The reaction mixture was cooled to rt, dissolved in DCM and passed through a silica plug to remove the zinc and Pd-catalyst. The solvent was evaporated using rotary evaporation, the crude residue was again dissolved in DCM and passed through a second silica plug followed by elution with DCM to ensure total removal of zinc and Pd-catalyst. The DCM was removed and the crude solid was isolated via precipitation from methanol. The solid was purified by boiling in isopropanol for 1.5 h followed by vacuum filtration, and washing with isopropanol (IPA). The product was again re-dissolved in DCM and slurried with Celite 545 and aluminum oxide for 1 h. The slurry was vacuum filtered and washed with DCM, after removal of solvent got red solid, in which methanol was added. The pure product (red solid) was isolated *via* vacuum filtration with methanol washing (0.557 g, 41% yield). This fraction of product was utilized for OLEDs device fabrication.

Note: It is important to note that **PDI-2** product has good solubility in MeOH and IPA, therefore the precipitation and washing steps were performed carefully. Both MeOH and IPA filtrates were combined and purified by flash column chromatography (Hexane /EtOAc = 95/05) using silica gel to give second fraction of **PDI-2** product (0.366 g, 27% yield), but this fraction of product showed small impurities in ¹H-NMR. This fraction was not used for OLEDs device fabrication.

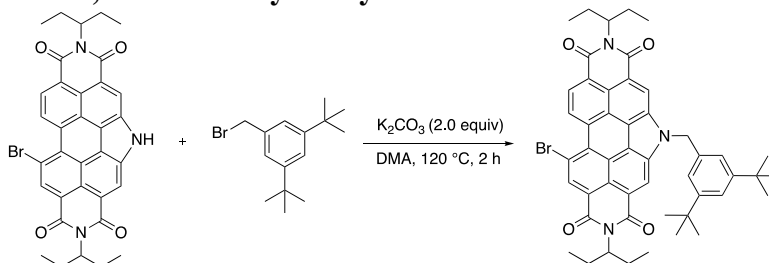
¹H-NMR (600 MHz, CDCl₃) δ: 8.83 (s, 2H), 8.66 (bs, 2H), 8.48 (bs, 2H), 7.96-7.94 (m, 2H), 7.71 (d, *J* = 8.4 Hz, 2H), 7.36 (s, 4H), 6.30 (s, 4H), 5.18 (bs, 2H), 5.01 (bs, 2H), 3.42-3.36 (m, 4H), 3.16-3.09 (m, 2H), 2.31 (bs, 4H), 2.16 (bs, 4H), 2.01-1.94 (m, 4H), 1.88-1.81 (m, 4H), 1.44 (d, *J* = 7.0 Hz, 12H), 1.22-1.21 (m, 24H), 0.99 (t, *J* = 7.5 Hz, 12H), 0.81 (bs, 12H).

¹³C-NMR (150 MHz, CDCl₃) δ: 151.56, 149.08, 140.91, 135.66, 135.44, 132.98, 130.42, 126.81, 125.19, 124.99, 124.80, 123.57, 122.77, 122.43, 120.28, 119.99, 57.94, 57.57, 44.69, 34.86, 30.46, 25.25, 25.12, 24.40, 24.25, 11.63, 11.38.

MALDI-TOF: (*m/z*) calculated [M-2H]⁺ for C₁₀₀H₁₀₄N₆O₈: 1515.7832, obtained: 1515.7867

Elemental Analysis: Theory %C 79.13, %H 6.91, %N 5.54. Actual %C 78.06, %H 6.71, %N 5.51.

Synthesis of Br-PDIN-3,5-di-tert-butylbenzyl:



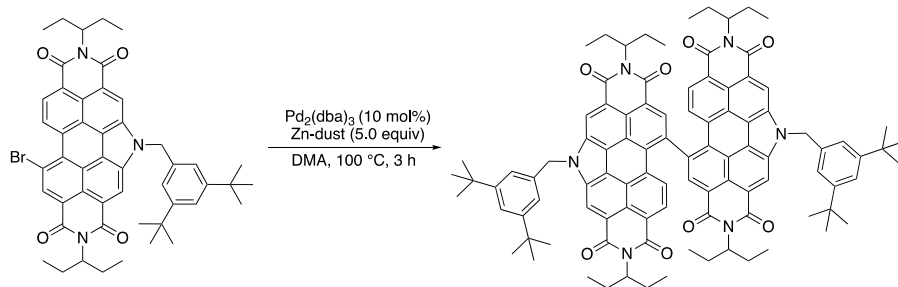
To a screw-capped vial equipped with a magnetic stir bar were added the **Br-PDIN-H** (1.0 g, 1.60 mmol), **1-(bromomethyl)-3,5-di-tert-butylbenzene** (0.592 g, 2.08 mmol), and K_2CO_3 (0.443 g, 3.21 mmol). The screw-capped vial was closed and evacuated using high vacuum, then refilled with nitrogen gas in three cycles. To the vial 8.0 mL of *N,N*-Dimethylacetamide (DMA) solvent was added using syringe under nitrogen and reaction mixture purged with nitrogen for 10 minutes. The reaction mixture was placed in heating block with stirring and heated to 120 °C. TLC analysis showed reaction completion after 2 h, then the reaction mixture was cooled to rt and dissolved in 200 mL of DCM and washed with water (3 X 400 mL). The solvent was evaporated using rotary evaporation and the crude residue was again dissolved in DCM and passed through silica plug followed by elution with DCM. The DCM was removed and the product was recrystallized by dissolving in a minimal amount of DCM and precipitating with MeOH. The pure product was isolated *via* vacuum filtration, washing with methanol (1.218 g, 92% yield).

1H -NMR (600 MHz, $CDCl_3$) δ : 10.10-10.06 (m, 1H), 8.99 (s, 1H), 8.94-8.93 (m, 2H), 8.82 (s, 1H), 7.38 (t, $J = 1.8$ Hz, 1H), 7.16 (s, 2H), 6.04 (s, 2H), 5.23-5.15 (m, 2H), 2.40-2.30 (m, 4H), 2.08-1.99 (m, 4H), 1.22 (s, 18H), 1.01-0.97 (m, 12H).

^{13}C -NMR (150 MHz, $CDCl_3$) δ : 152.12, 134.88, 134.67, 134.45, 132.12, 130.21, 127.30, 124.15, 123.45, 123.22, 122.84, 121.92, 121.59, 121.29, 118.72, 118.32, 58.21, 58.07, 51.11, 34.97, 31.43, 25.34, 25.29, 11.73, 11.69.

MALDI-TOF: (m/z) calculated $[M-2H]+H^+$ for $C_{49}H_{50}BrN_3O_4$: 822.2901, obtained: 822.2868

Synthesis of PDI-3:



To a 40 mL screw-capped vial equipped with a magnetic stir bar were added the **Br-PDIN-3,5-di-tert-butylbenzyl** (1.1 g, 1.33 mmol), **zinc dust** (0.436 g, 6.67 mmol), and **Pd₂(dba)₃** (0.122 g, 0.13 mmol) inside the glove box and the vial was closed with a cap. The mixture was dissolved in 20.0 mL of DMA solvent outside the glove box under nitrogen. The reaction mixture was placed in heating block with stirring and heated to 120 °C, after which the solution turned blue. TLC analysis showed completion of reaction after 3 h. The reaction mixture was cooled to rt, dissolved in DCM and passed through a silica plug to remove the zinc and Pd-catalyst. The solvent was evaporated using rotary evaporation, the crude residue was again dissolved in DCM and passed through a second silica plug followed by elution with DCM to ensure total removal of zinc and Pd-catalyst. The DCM was removed and the crude solid was isolated via precipitation from methanol. The solid was purified by boiling in isopropanol for 1.5 h followed by vacuum filtration, and washing with isopropanol. The product was again re-dissolved in DCM and slurried with Celite 545 and aluminum oxide for 1 h. The slurry was vacuum filtered and washed with DCM, after removal of solvent got red solid, in which methanol was added. The pure product (red solid) was isolated *via* vacuum filtration with methanol washing (0.804 g, 81% yield).

¹H-NMR (600 MHz, CDCl₃) δ: 9.23 (s, 2H), 9.06 (s, 2H), 8.87 (bs, 2H), 8.01 (d, *J* = 8.1 Hz, 2H), 7.77 (d, *J* = 8.4 Hz, 2H), 7.48 (t, *J* = 1.8 Hz, 2H), 7.36 (bs, 4H), 6.19 (s, 4H), 5.21 (bs, 2H), 5.03 (bs, 2H), 2.34 (bs, 4H), 2.19 (bs, 4H), 2.02-1.95 (m, 4H), 1.89-1.82 (m, 4H), 1.32 (s, 36H), 1.00 (t, *J* = 7.4 Hz, 12H), 0.82 (bs, 12H).

¹³C-NMR (150 MHz, CDCl₃) δ: 152.29, 141.07, 135.70, 135.48, 135.18, 133.16, 130.61, 127.07, 125.16, 124.96, 123.79, 123.01, 122.97, 121.95, 120.50, 120.22, 58.09, 57.71, 51.54, 35.10, 31.55, 25.31, 25.17, 11.62, 11.36.

MALDI-TOF: (*m/z*) calculated [M-2H]⁺H⁺ for C₉₈H₁₀₀N₆O₈: 1487.7519, obtained: 1487.7568

Elemental Analysis: Theory %C 79.00, %H 6.77, %N 5.64. Actual %C 78.38, %H 6.98, %N 5.72.

NMR Spectroscopy:

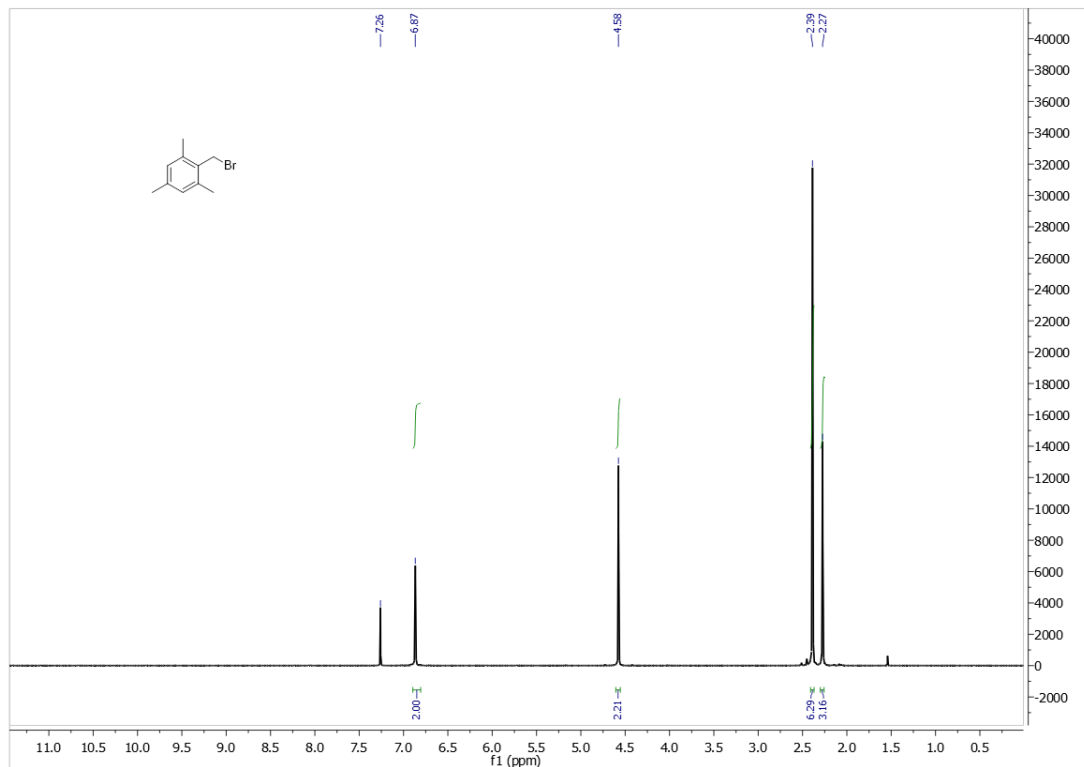


Figure S4: $^1\text{H-NMR}$ spectrum of 1-(bromomethyl)-2,4,6-trimethylbenzene in CDCl_3

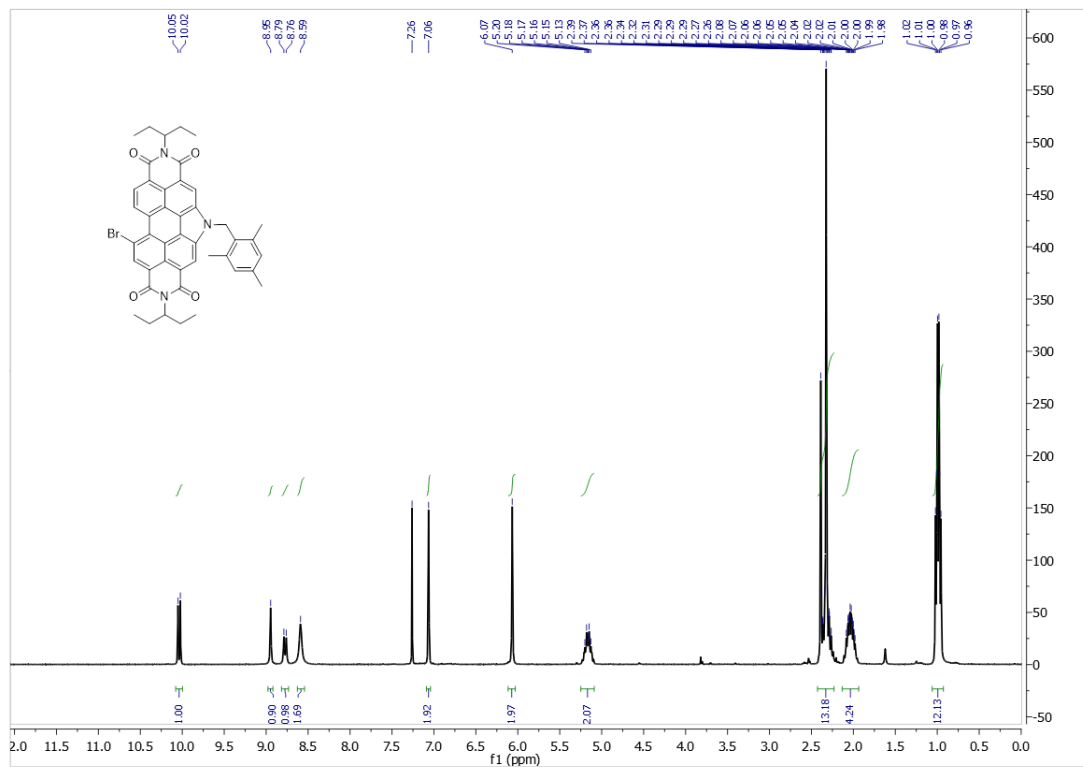


Figure S5: $^1\text{H-NMR}$ spectrum of Br-PDIN-2,4,6-trimethylbenzyl in CDCl_3

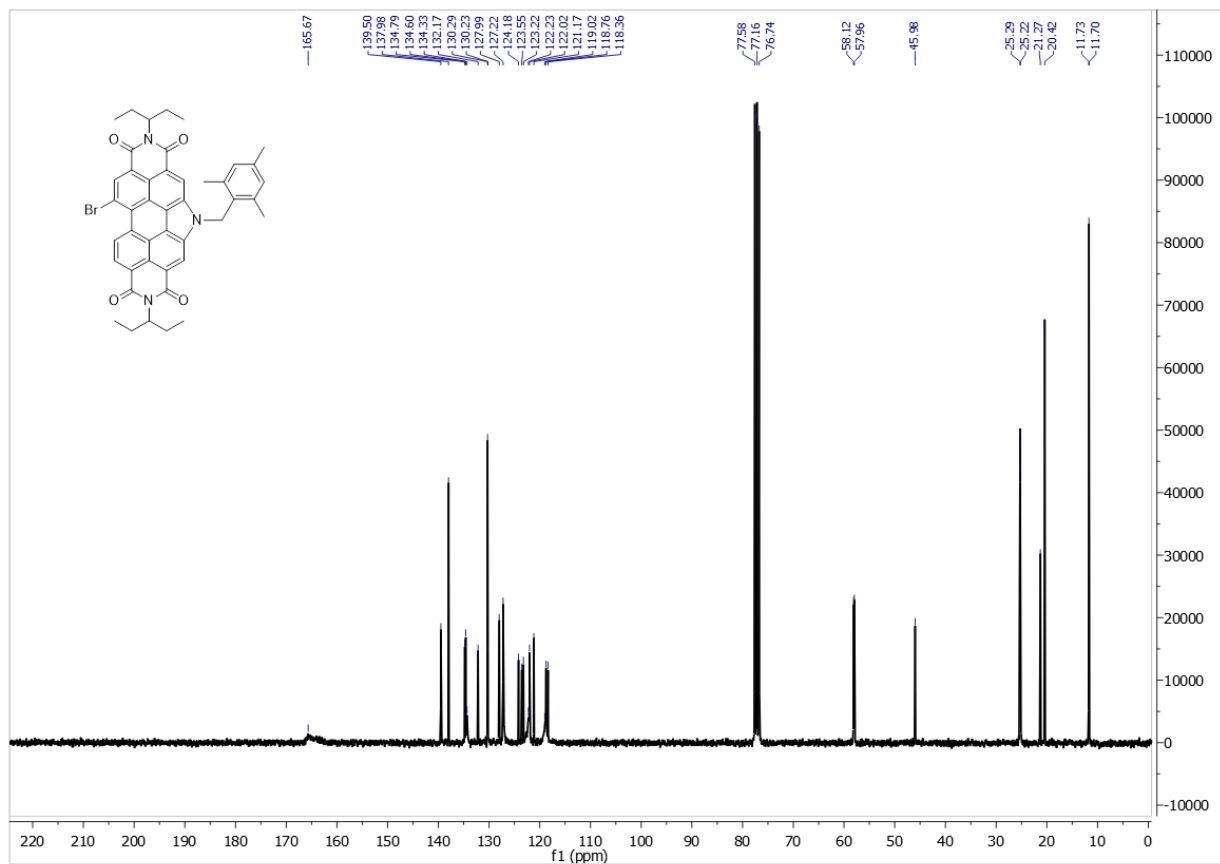


Figure S6: ^{13}C NMR spectrum of Br-PDIN-2,4,6-trimethylbenzyl in CDCl_3

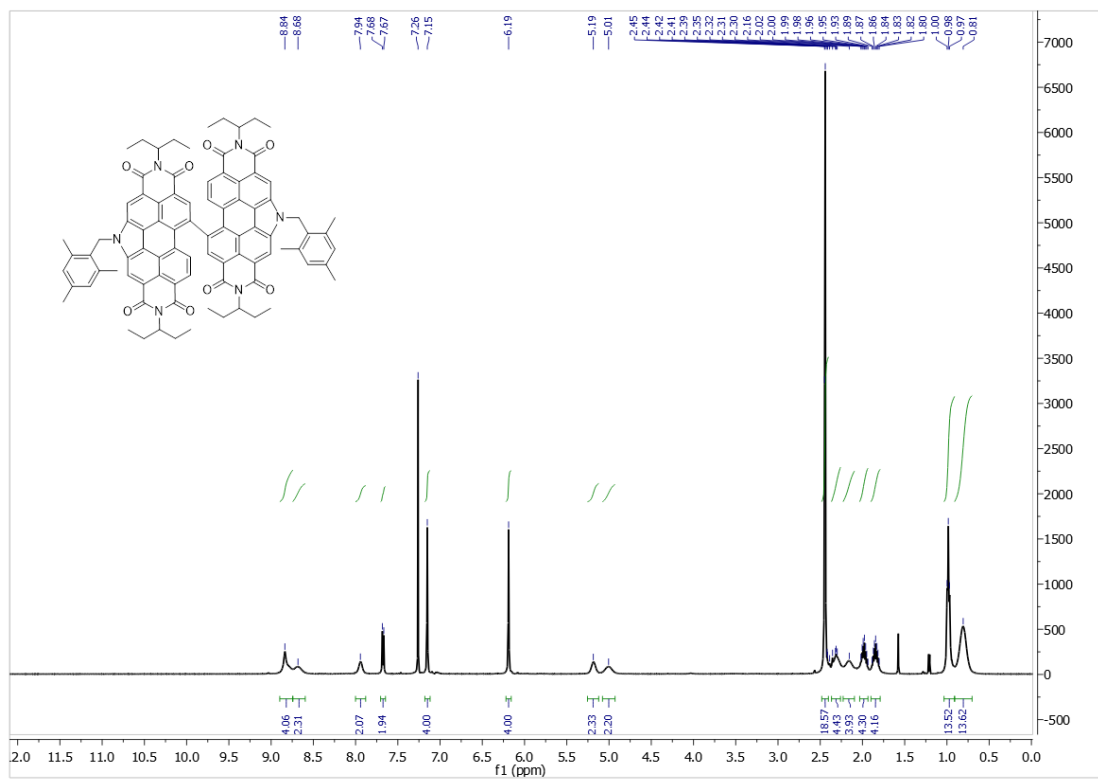


Figure S7: $^1\text{H-NMR}$ spectrum of PDI-1 in CDCl_3

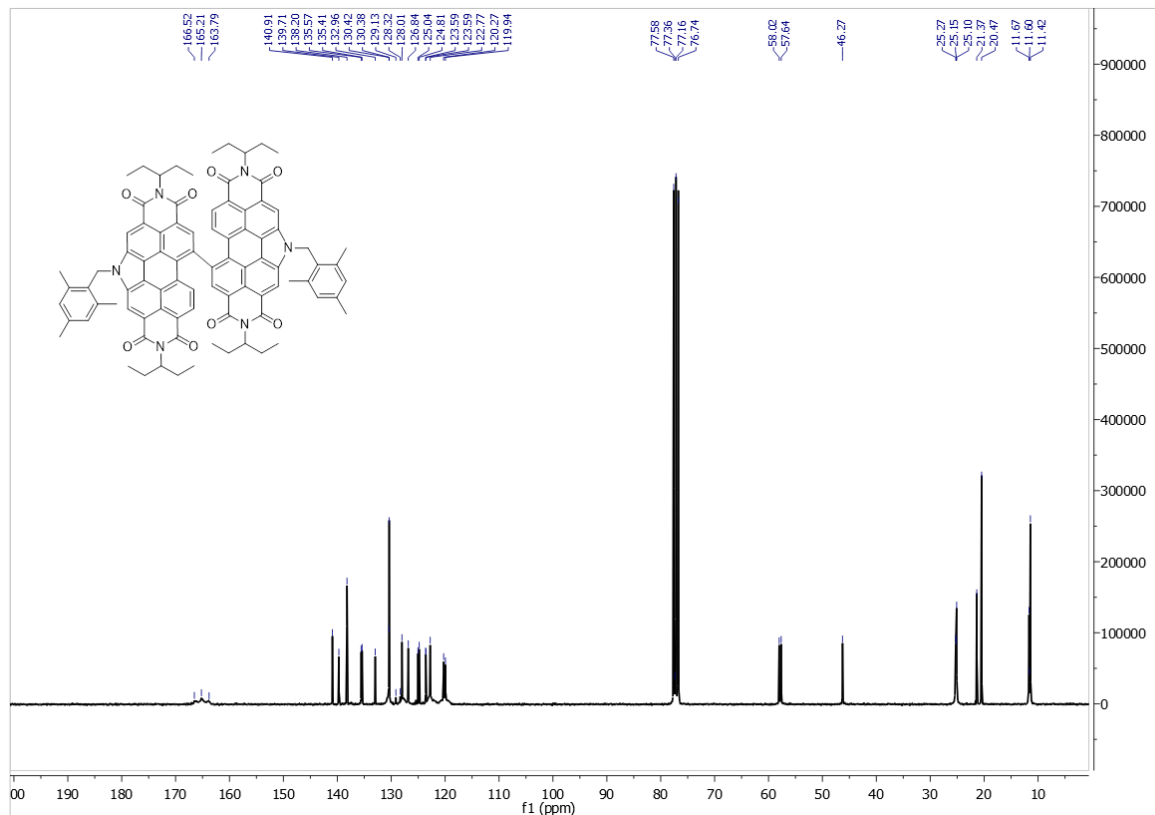


Figure S8: ¹³C NMR spectrum of PDI-1 in CDCl₃

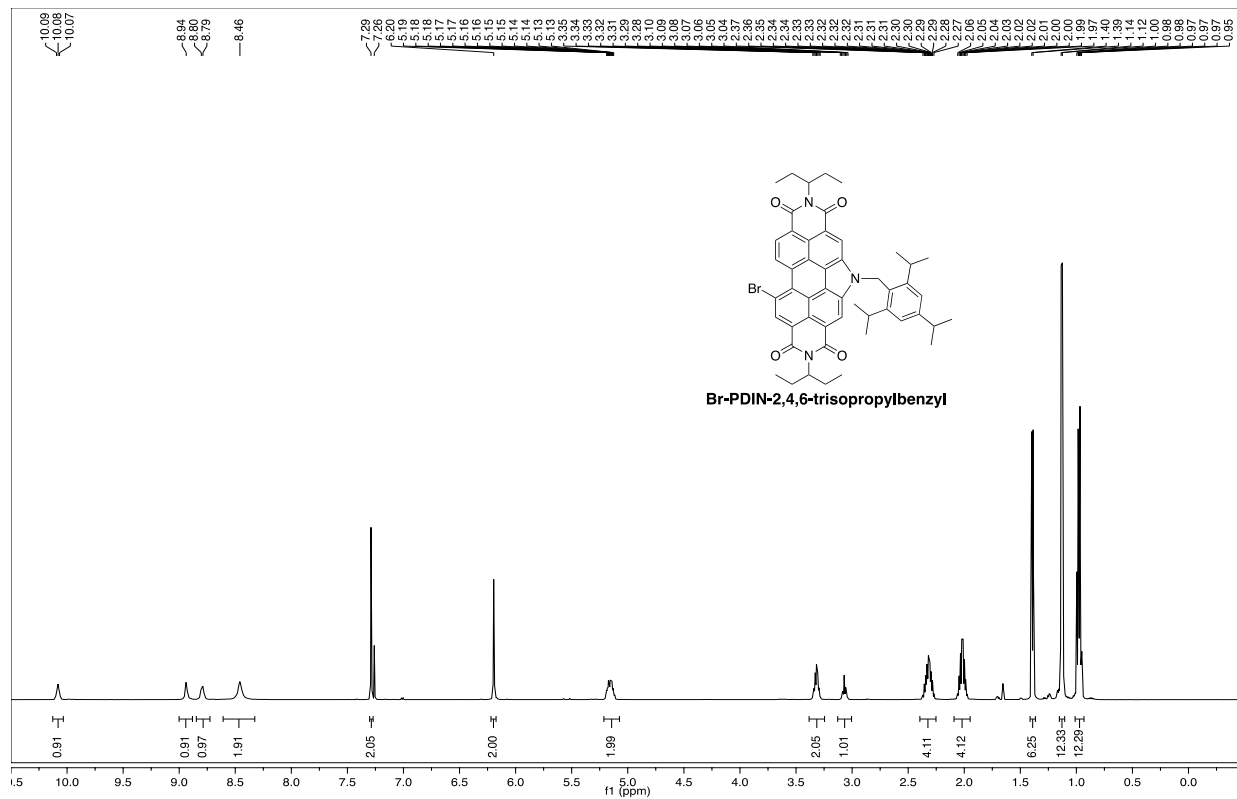


Figure S9: $^1\text{H-NMR}$ spectrum of Br-PDIN-2,4,6-trisopropylbenzyl in CDCl_3

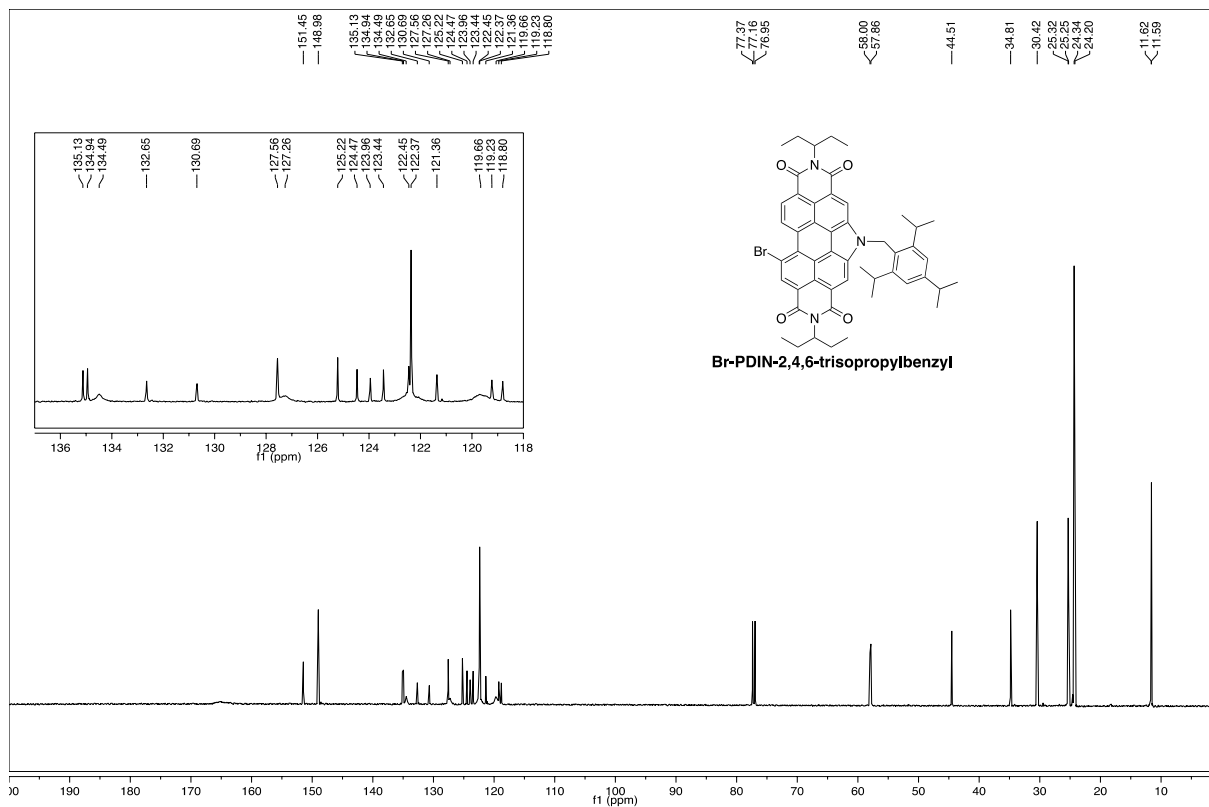


Figure S10: ^{13}C -NMR spectrum of Br-PDIN-2,4,6-trisopropylbenzyl in CDCl_3

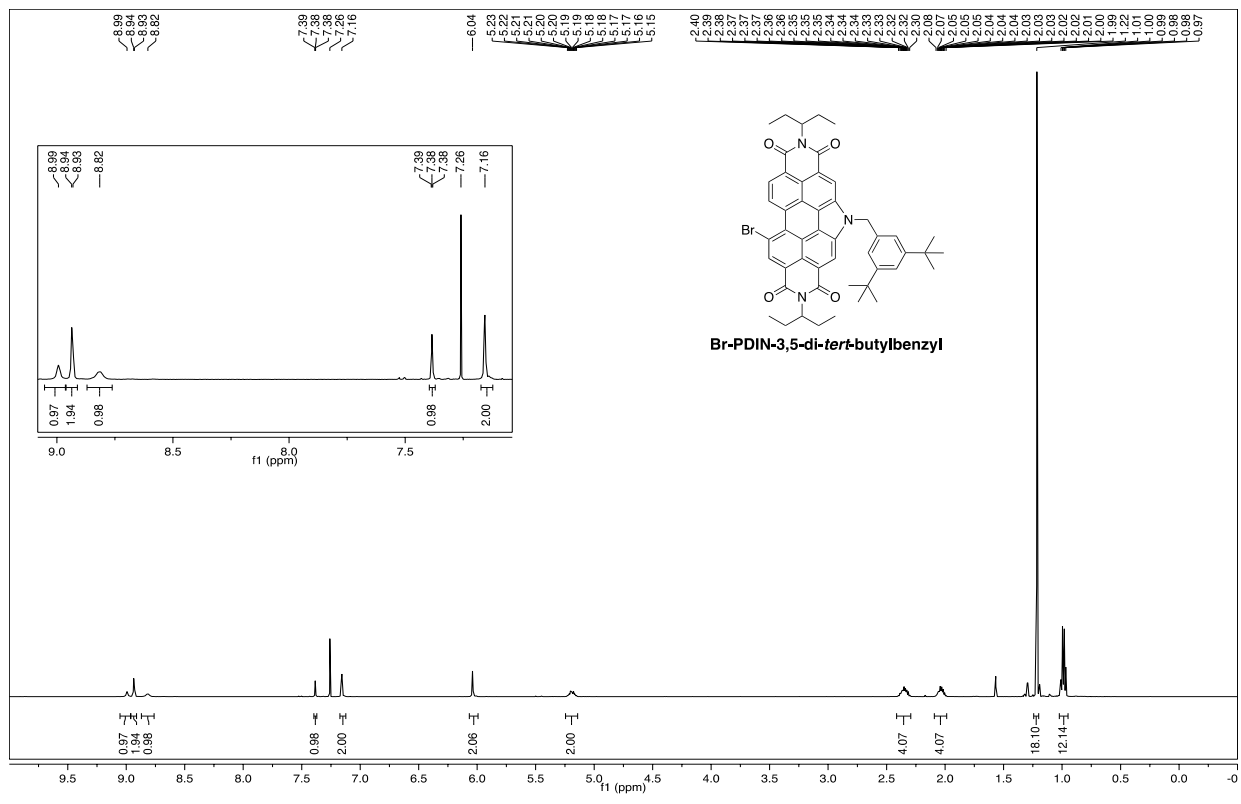


Figure S11: $^1\text{H-NMR}$ spectrum of Br-PDIN-3,5-di-*tert*-butylbenzyl in CDCl_3

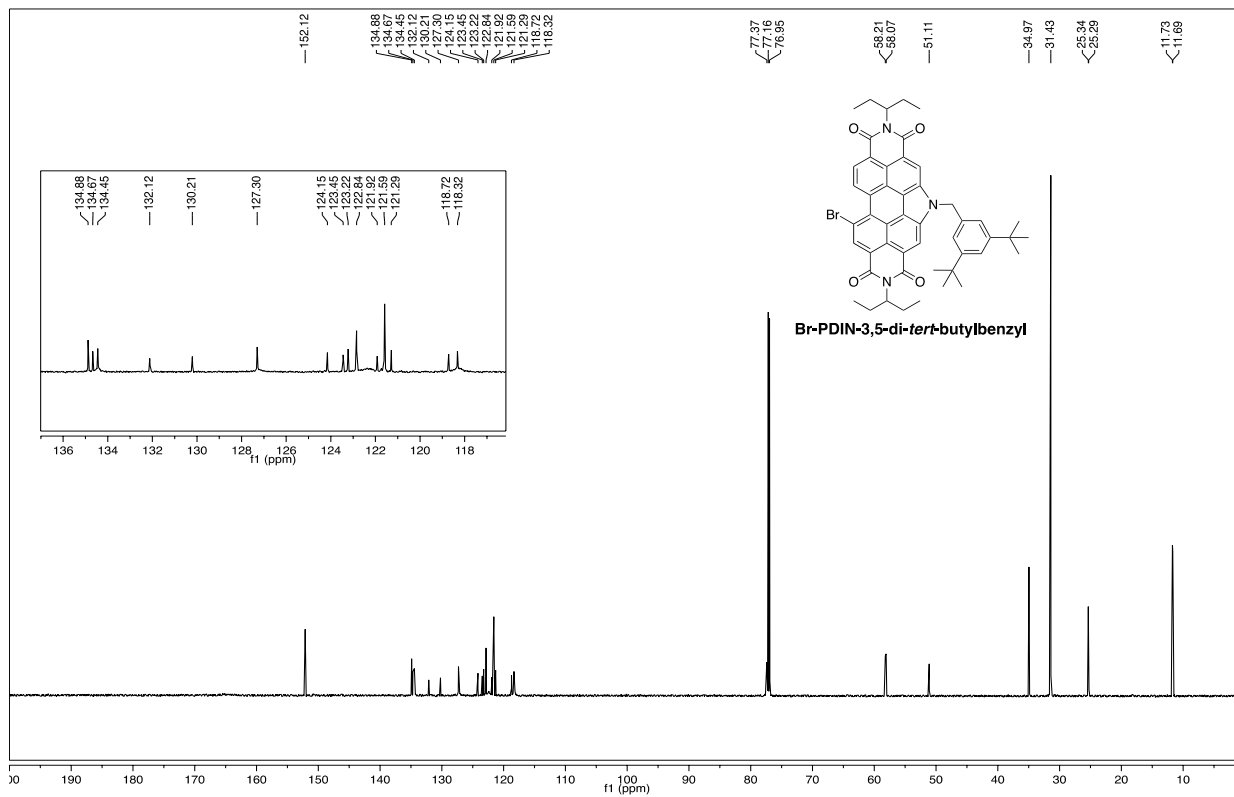


Figure S12: $^{13}\text{C-NMR}$ spectrum of Br-PDIN-3,5-di-*tert*-butylbenzyl in CDCl_3

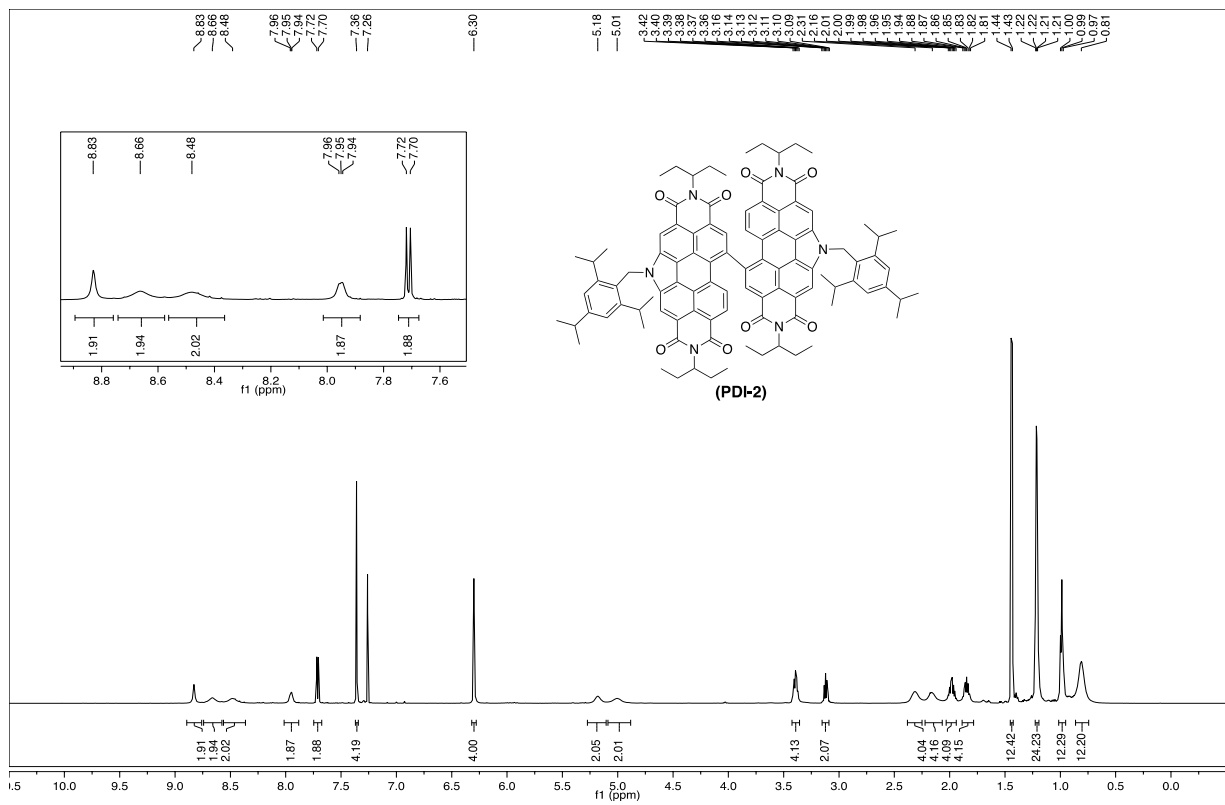


Figure S13: ¹H-NMR spectrum of PDI-2 in CDCl₃

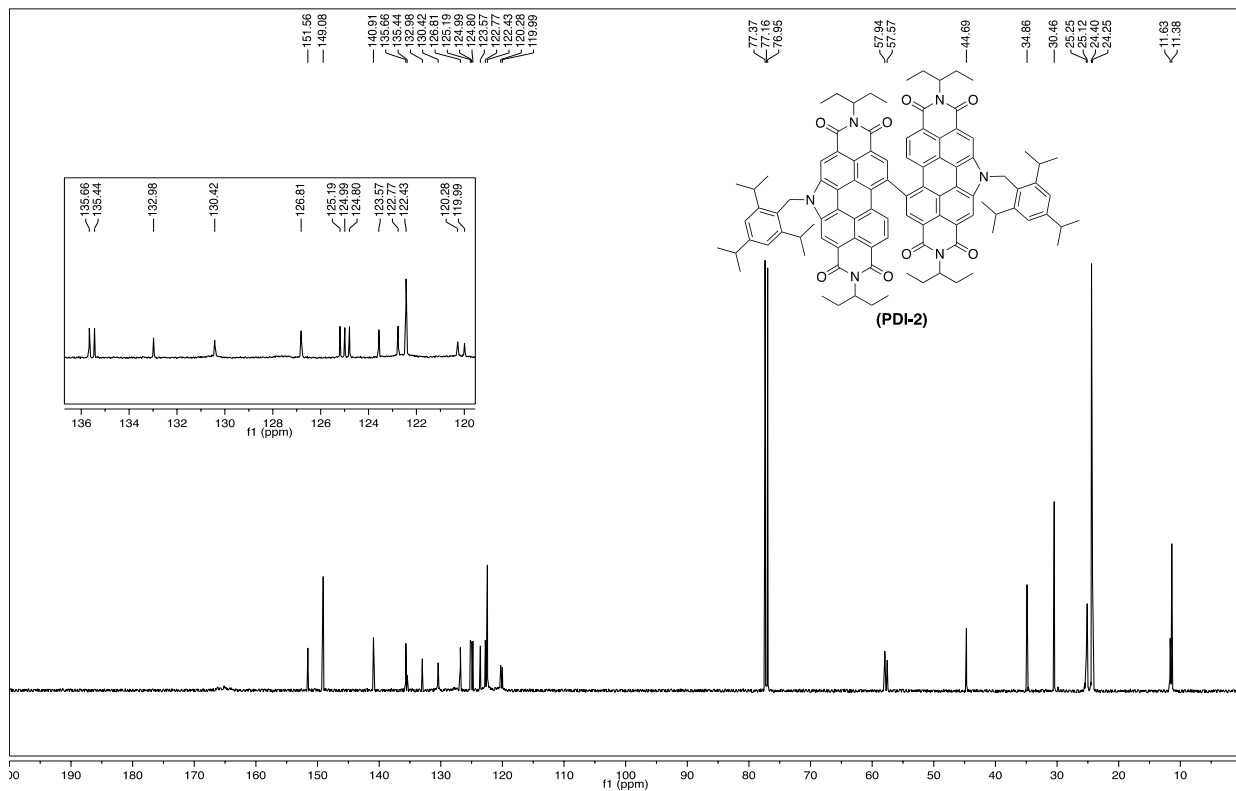


Figure S14: ^{13}C -NMR spectrum of PDI-2 in CDCl_3

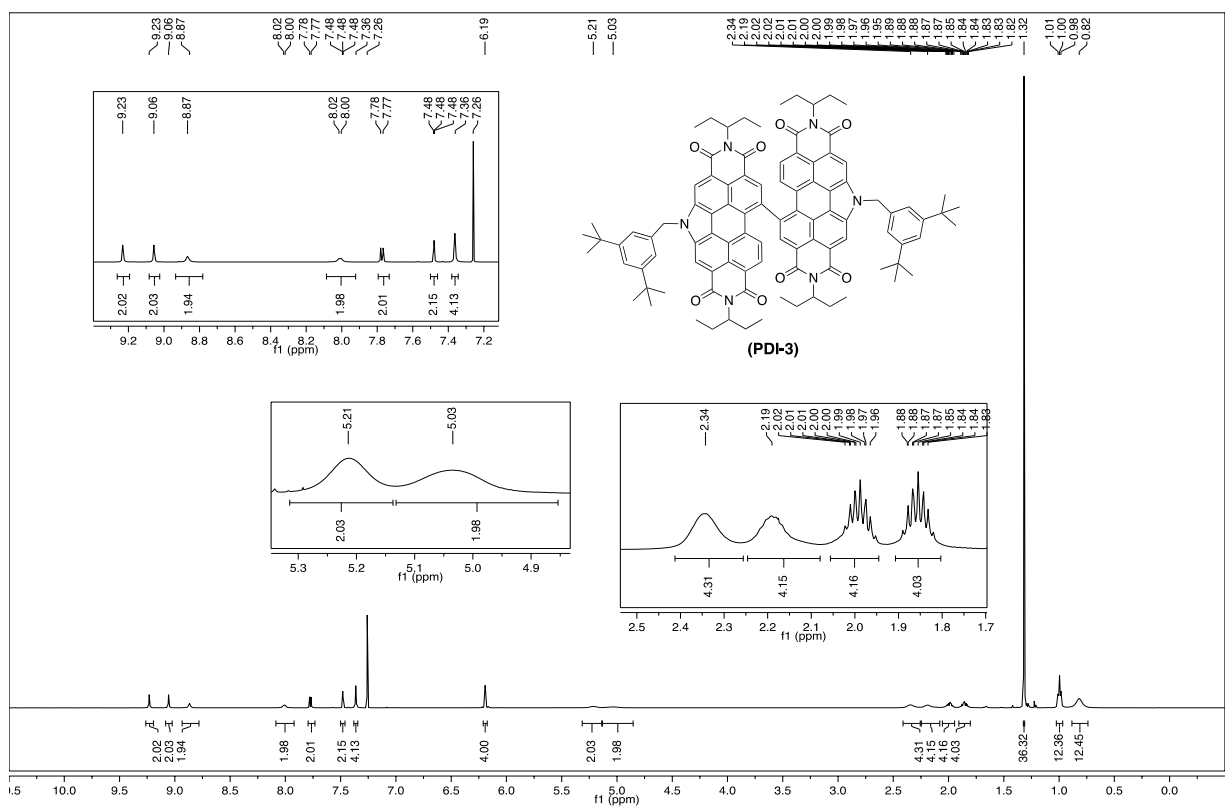


Figure S15: $^1\text{H-NMR}$ spectrum of PDI-3 in CDCl_3

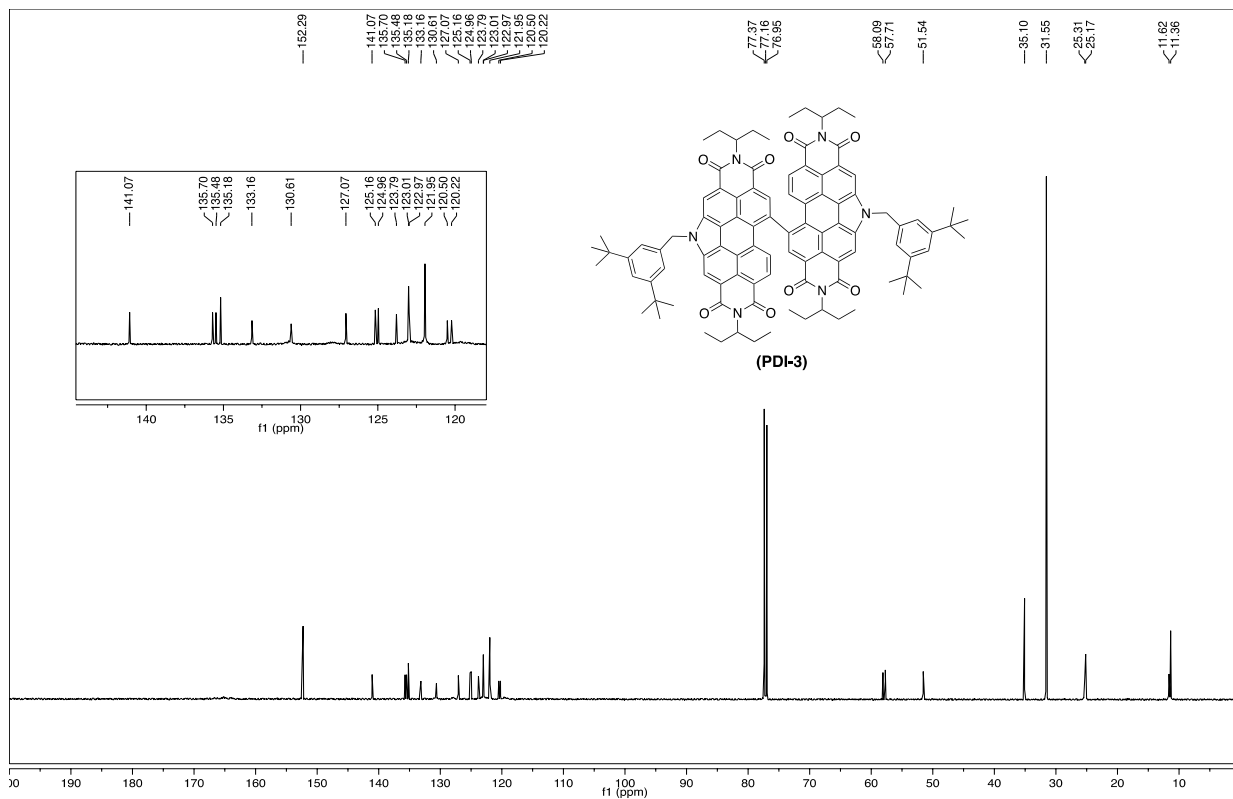


Figure S16: ^{13}C -NMR spectrum of PDI-3 in CDCl_3

Mass Spectrometry Spectra:

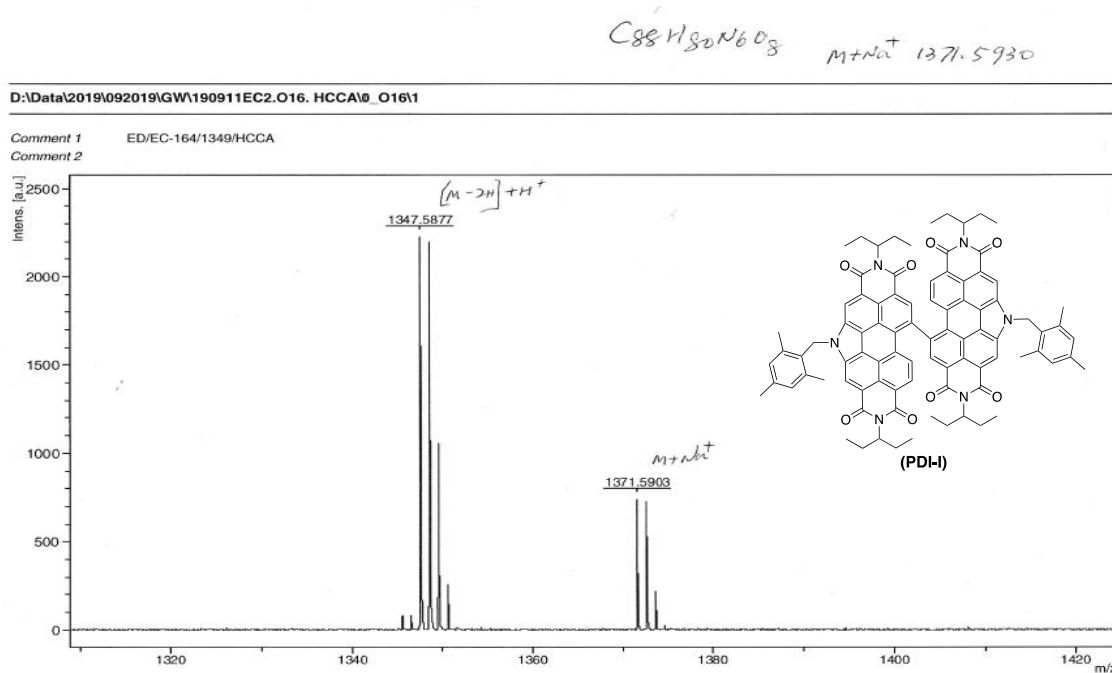


Figure S17: MALDI-TOF spectra of PDI-1

Compound
 $C_{100}H_{104}N_{6}O_8$ (M-2H)⁺ 1515.783

D:\Data\2020\2006\JVH\200624SB4.G12.HCCA\0_K12\1

Comment 1 SACHIN/I-46/1516/HCCA
Comment 2

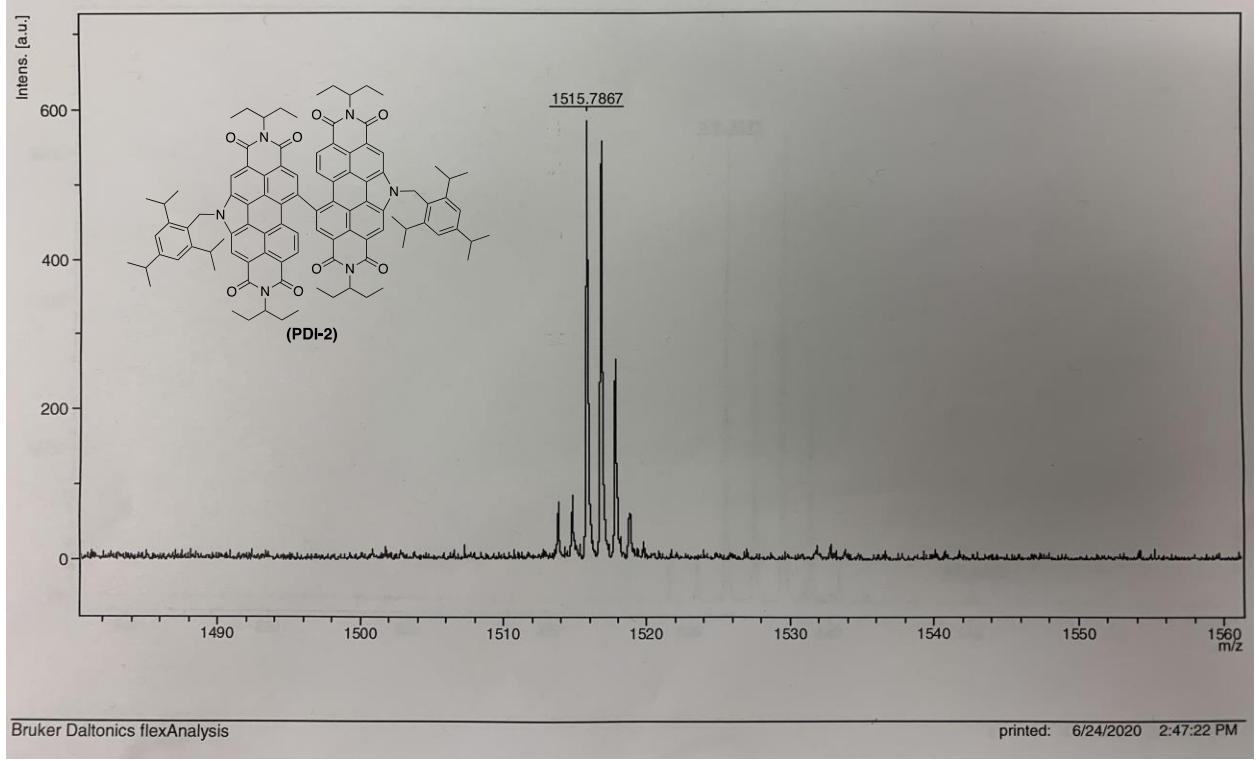


Figure S18: MALDI-TOF spectra of PDI-2

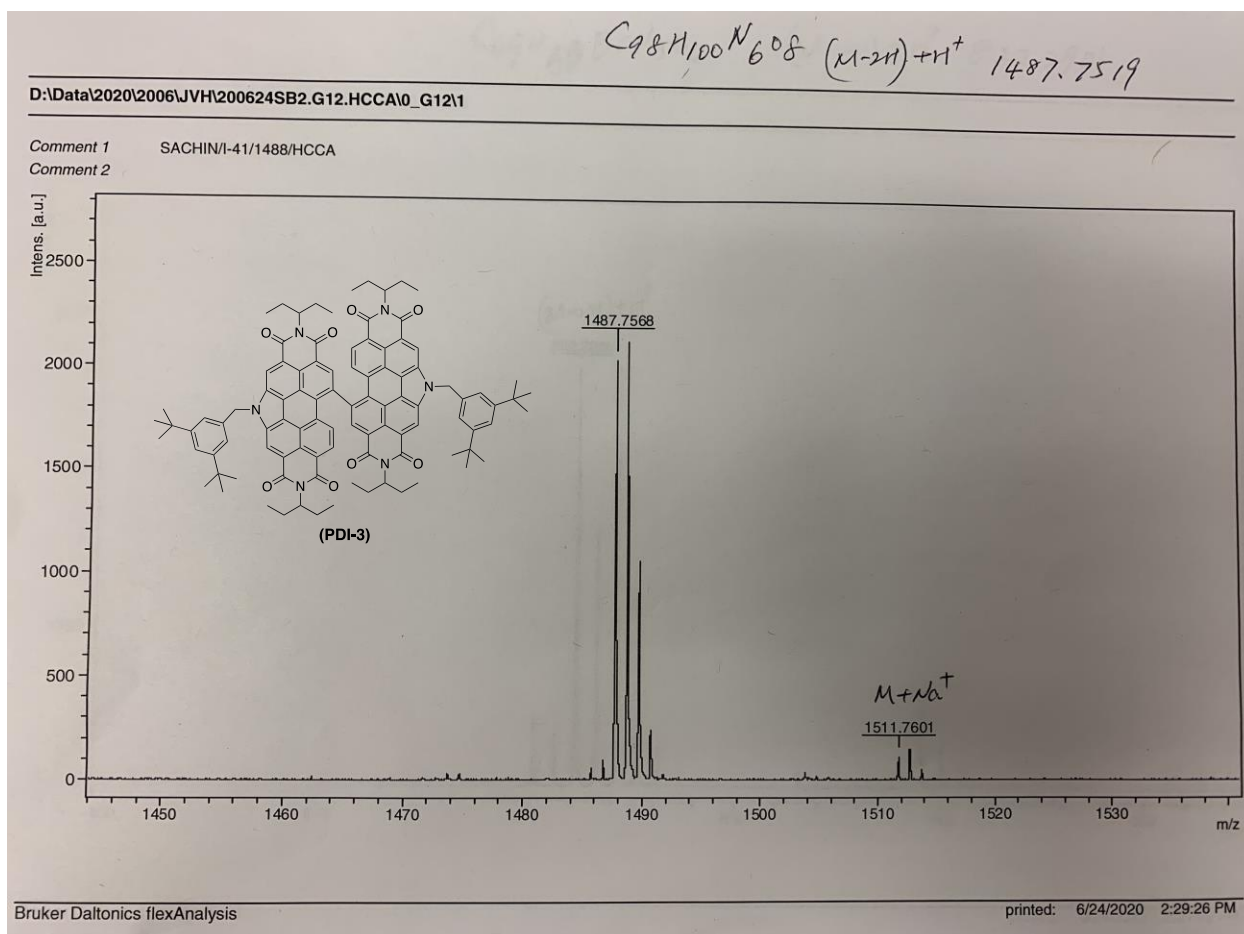


Figure S19: MALDI-TOF spectra of PDI-3

Electrochemistry

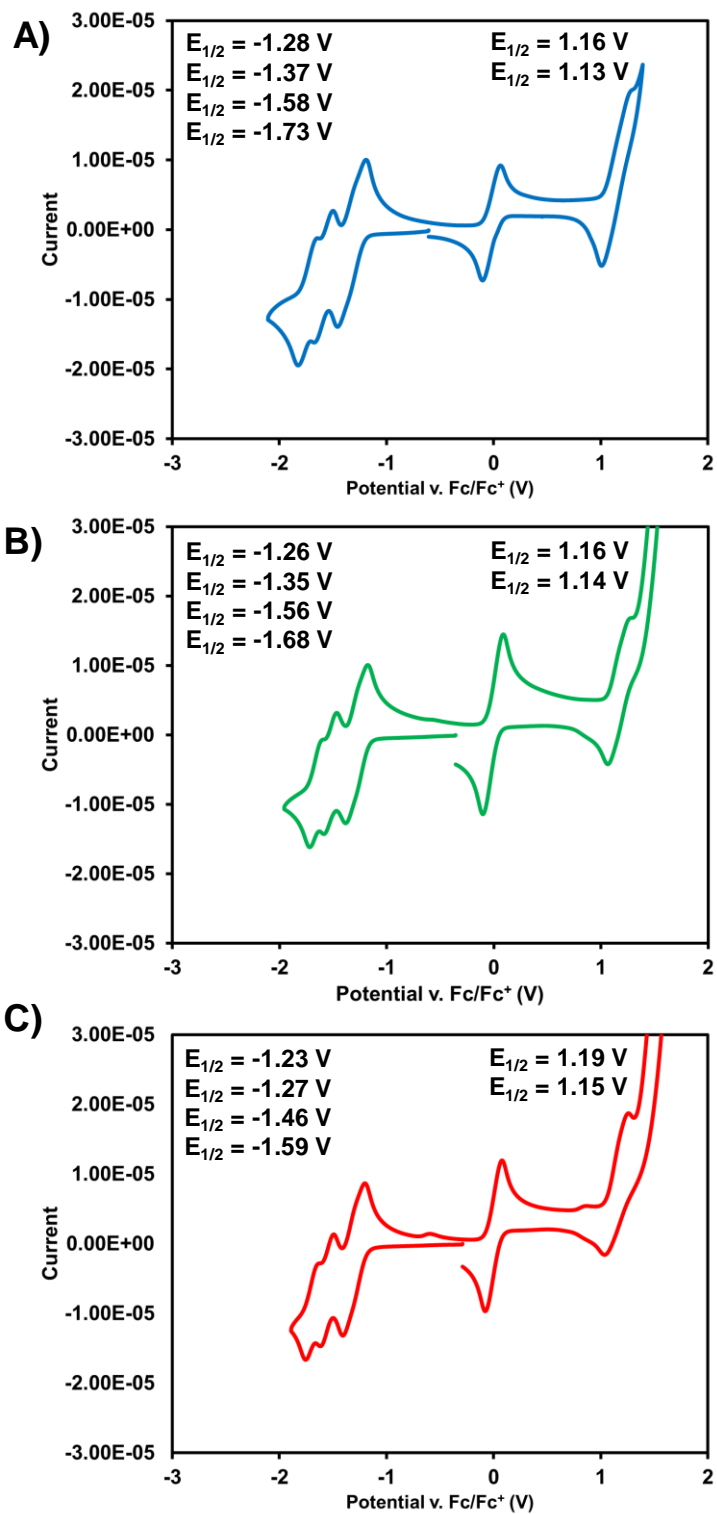


Figure S20. CV plots for PDI-1 (A), PDI-2 (B), and PDI-3 (C). CV experiments run in CH₂Cl₂ solution.

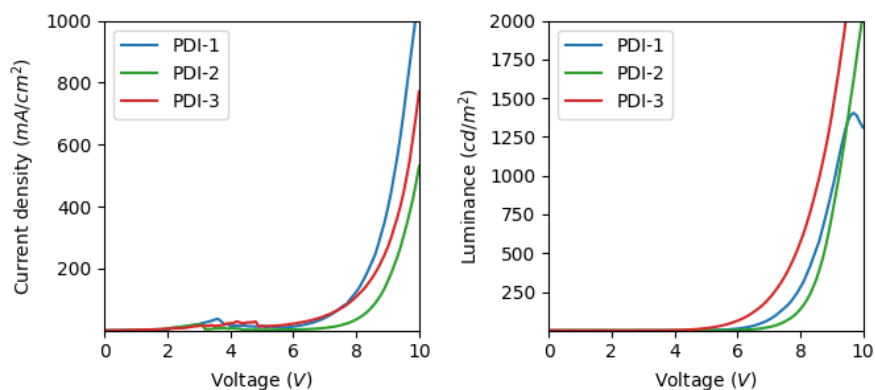


Figure S21. Plots of current-voltage (left) and luminance-voltage (right) for OLEDs based on PDI-1, PDI-2, and PDI-3.

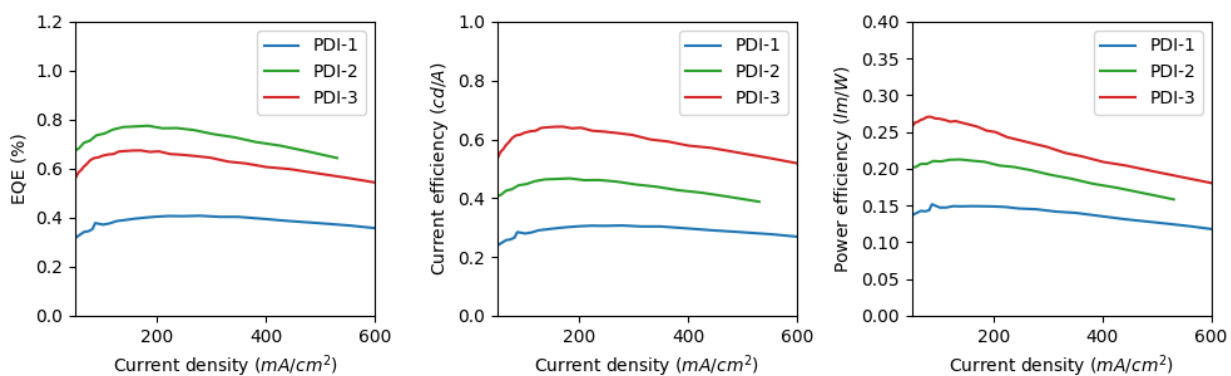


Figure S22. Plots of EQE-current density (left), current efficiency-current density (center), and power efficiency-current density for OLEDs based on PDI-1, PDI-2, and PDI-3.

References

1. Nazari, M. *et al.* Benzyl and fluorinated benzyl side chains for perylene diimide non-fullerene acceptors. *Mater. Chem. Front.* **2**, 2272–2276 (2018).
2. Handa, S., Andersson, M. P., Gallou, F., Reilly, J. & Lipshutz, B. H. Handa. Phos: A General Ligand Enabling Sustainable ppm Levels of Palladium-Catalyzed Cross-Couplings in Water at Room Temperature. *Angew. Chemie Int. Ed.* **55**, 4914–4918 (2016).
3. Niehues, M. *et al.* Structural characterization of Group 4 transition metal halide bis-Arduengo carbene complexes MC14L2: *J. Organomet. Chem.* **663**, 192–203 (2002).
4. Qian, L. *et al.* Electroluminescence from light-emitting polymer/ZnO nanoparticle heterojunctions at sub-bandgap voltages. *Nano Today* **5**, 384–389 (2010).
5. Forrest, S. R., Bradley, D. D. C. & Thompson, M. E. Measuring the Efficiency of Organic Light-Emitting Devices. *Adv. Mater.* **15**, 1043–1048 (2003).
6. Anaya, M. *et al.* Best practices for measuring emerging light-emitting diode technologies. *Nat. Photonics* **13**, 818–821 (2019).
7. Würth, C., Grabolle, M., Pauli, J., Spieles, M. & Resch-Genger, U. Relative and absolute determination of fluorescence quantum yields of transparent samples. *Nat. Protoc.* **8**, 1535–1550 (2013).